J Mol Model (2009) 15:469–479
DOI 10.1007/s00894-008-0432-7

ORIGINAL PAPER

Systematic characterization on electronic structures and spectra for a series of complexes, $M(IDB)Cl_2$ (M = Mn, Fe, Co, Ni, Cu and Zn): a theoretical study

Yanyan Zhu · Zhanfen Chen · Zijian Guo · Yan Wang · Guangju Chen

Received: 6 October 2008 / Accepted: 17 November 2008 / Published online: 13 December 2008

Abstract Theoretical studies on the coordination stabilities, spectra and DNA-binding trend for the series of metal-varied complexes, $M(IDB)Cl_2$ (M = Mn, Fe, Co, Ni, Cu and Zn; IDB = N, N -bis(2-benzimidazolylmethyl) amine), have been carried out by using the DFT/B3LYP method and PCM model. The calculated coordination stabilities (S) for these complexes present a trend of S(Ni) > S(Co) > S(Fe) > S(Cu) > S(Zn) > S(Mn). It has been estimated from the molecular orbital energies of the complexes that the DNA-binding affinities (A) of the complexes are in the order of A(Zn) < A (Mn) < A(Fe) ≈ A(Co) < A(Ni) < A(Cu). The studied results indicate that the Cu, Ni and Co complexes with large coordination stabilities present the low virtual orbitals, consequently yielding to the favorable DNA-binding affinities. The spectral properties of excitation energies and oscillator strengths for $M(IDB)Cl_2$ in the ultraviolet region were calculated by TD-DFT/B3LYP method.

Keywords Coordination stability · DFT/B3LYP · IDB · Spectra · TD-DFT · Transition metals

Y. Zhu · Y. Wang (✉) · G. Chen (✉)
College of Chemistry, Beijing Normal University,
19# Xinjiekouwai street, Haidian district,
Beijing 100875, People's Republic of China
e-mail: wangy@bnu.edu.cn
e-mail: gjchen@bnu.edu.cn

Z. Chen · Z. Guo
State Key Laboratory of Coordination Chemistry,
School of Chemistry and Chemical Engineering,
Nanjing University,
Nanjing 210093, People's Republic of China

Introduction

Transition metal complexes have attracted considerable attention, during the past decades, for their potential utilities in nucleic acid probes [1–8], DNA-molecular light switches [9–12], anti-HIV drugs [13], DNA sequence-specific cleaving agents [14–21] and so on. A great deal of interest has been concentrated on the functional molecule design of transition metal complexes in order to improve DNA-binding/DNA-cleaving activities [7, 8]. Recently, a great number of transition metal complexes with efficient interaction with DNA have been designed, synthesized and characterized as artificial nucleases [22–25]. Generally, these complexes can interact with double-stranded DNA in different ways [26, 27], in which there mainly are three types of binding modes, i.e., electrostatic binding mode, groove binding mode, and intercalative binding mode [28–31]. The study on electronic and structural properties for these transition metal complexes would provide a fundamental understanding of nuclease-DNA interaction, even though they are comparatively small and simple molecules [32–34].

The selective binding and damaging properties of DNA by transition metal complexes were investigated by a great number of experiments in the past years [35–37]. The extensive investigations by Barton and coworkers has demonstrated that the intercalative ligand should generally contain a functional aromatic heterocycle inserting and stacking between the base pairs of double helical DNA [3, 4, 7–9, 38–47]. For instance, the first copper complex representing the efficient interaction with DNA is bis (1,10-phenanthroline)copper(I) [48, 49] that includes a phen-heterocycle. Recently, the metal complexes with benzimidazole and its derivative ligands, such as IDB (*N*, *N* -bis(2-benzimidazolylmethyl) amine), is particularly

attractive for developing new diagnostic and therapeutic agents due to their synthetic accessibility and high binding affinities to DNA [50–52]. A rigid aromatic ring presented in the benzimidazole structure can selectively interact with a specific DNA sequence, which makes the benzimidazole unit remain a stable conformation that provides an appropriate platform to build further DNA sequence recognition [53–60]. Furthermore, such an aromatic ring stacking the deoxyribonucleic acid base pairs in DNA molecule is considered to be a major driving force to bind to DNA [3, 14]. It is clear from the previous studies that the nuclease activities of transition metal complexes can be modified by numerous factors, such as coordination environment of metal ions, ligand structure, and nuclearity [34]. Especially, in comparison to the 4 d- or 5 d-metal analogues, the complexes with first row transition metals have also been found to present the nucleic reactivity and great applications at the cellular level. Wang et al. [22] have reported that the catalytic activities upon the interactions of different central metals, such as zinc(II), copper (II), cobalt(II), in the mononuclear complexes with DNA are notably different; namely the copper complex is a better catalyst in the DNA damage process than the zinc and cobalt complexes. Kang et al. [23] have given a similar observation that the catalytic activity of the copper(II) complex is fast, simple and efficient.

It should be a difficult subject, however, to essentially understand the interaction mechanisms of transition metal complexes with DNA double strands unless we can obtain more detailed information at a molecular level. The theoretical chemists have been interested in investigating the catalytic properties of transition metal complexes for biological systems by using theoretical calculations [61–66] in more recent years. These theoretical explorations on the electronic structures and active properties of the complexes are very significant in guiding the analysis of the DNA-binding and DNA-damage mechanisms [61, 62, 64–69]. For instance, the difference in DNA-binding affinities of the two novel chiral Ru(II) complexes can be reasonably explained by the frontier molecular orbital theory, i.e., the orbital interactions between the LUMOs (lowest unoccupied molecular orbital) of metal complexes and the HOMO (highest occupied molecular orbital) of DNA from the DFT calculations [62]. The trend in the binding constant (K_b) of $[M(phen)_3]^{2+}$ (M = Zn, Os and Ru) obtained from the theoretical calculations is in the order of $K_b(Zn) < K_b(Ru) < K_b(Os)$, which reproduces the experimental results [70]. However, due to interaction potential of nuclease with DNA in biological environment, the interaction mechanisms of first row transition metal complexes with DNA are still a controversial issue [71]. Especially, to the best of our knowledge, the systematically theoretical investigations on the electronic properties of the metal complexes including metal elements in the same period have been limited till now.

In the present work, we carried out the DFT/B3LYP calculations on the geometries, molecular orbitals, and electronic properties for the mononuclear complexes, M(IDB)Cl_2 (M = Mn, Fe, Co, Ni, Cu and Zn). In addition, the electronic absorption spectra of the complexes are also simulated and characteristically assigned with the DFT/TDDFT method. Our research goals are: 1) to find the relationships in the electronic properties of these transition metal complexes in the same period; and more importantly, 2) to understand how the properties of molecular orbitals of the series of transition metal complexes affect DNA-complex binding abilities.

Computational details

The component sketch of the investigated complexes, each of which has 39 atoms, is shown in Fig. 1(a). The geometries for the studied complexes, M(IDB)Cl_2 (M = Mn, Fe, Co, Ni, Cu and Zn), were fully optimized at the DFT/B3LYP [72–74] level of theory. The calculations were carried out with a mix basis set, i.e., 6-311G** basis set for C, N, Cl and H atoms, LanL2DZ, which has a relativistic effective core potential with a valence basis set, for Mn, Fe, Co, Ni, Cu and Zn atoms [75–77]. Furthermore, the extended basis set TZVP [78] has been employed for all atoms to calculate further the energies and orbital properties based on the optimized geometries of the studied complexes. This improvement of the basis set does not change the energies and orbital compositions by more than a percentage of six. Taking an acceptable computational cost into account, the mix basis set of 6-311G** +LanL2DZ was used for further calculations. The frequency calculations for these complexes were also carried out to verify the optimized structures to be energy minima without any

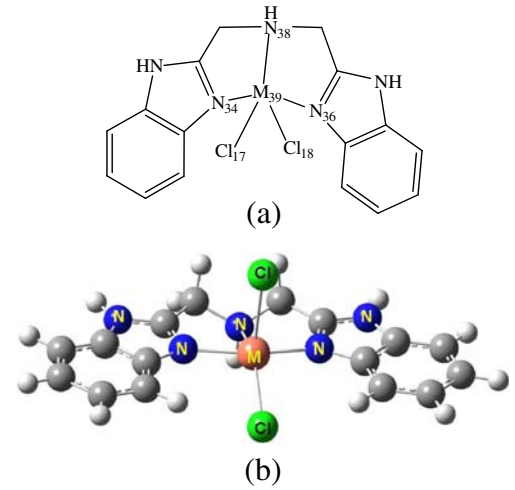

Fig. 1 Component sketch (**a**) and optimized geometry diagram (**b**) for M(IDB)Cl_2 (M = Mn, Fe, Co, Ni, Cu and Zn) complexes

imaginary frequency. Because the ligands of three N and two Cl ions around the central metal cations in the complexes cause a splitting of d orbital of the central transition metal cations mostly with a trigonal bipyramidal symmetry, the ground spin states verified computationally for the transition metal cations are Mn^{2+} (d^5) with doublet, Fe^{2+} (d^6) with triplet, Co^{2+} (d^7) with doublet, Ni^{2+} (d^8) with singlet, Cu^{2+} (d^9) with doublet and Zn^{2+} (d^{10}) with singlet in the present calculations. The ground-state multiplicities and first-excited energies have been shown in Table 1.

To understand the properties of these complexes, the solvent effect (methanol chosen from the available experiment [79]) is considered as an important factor. The polarized continuum model (PCM) [80] has been employed to simulate the solvent effects as implemented within the solvent reaction field using the optimized structures in the gas phase and in methanol solvent. In PCM, one divides the problem into a solute part (the complex) and a solvent part (methanol) represented as a structureless material characterized by its dielectric constant as well as other parameters.

The electronic properties of the complexes were studied using the natural bond orbital (NBO) analysis at the same level in methanol solvent by the NBO 3.1 program [81]. The time-dependent density functional theory (TD-DFT) methodology is a reliable tool for calculating the excited states for 3*d* transition metal systems with the open-shell electrons [82]. The energies and oscillator strengths with 80-130 lowest-energy electronic transitions, which involve the calculations of singlet-excited-state energies of the complexes, were computed by using TD-DFT method with the same basis sets in methanol solvent [83]. UV absorption spectra including all calculated transitions were simulated with the GaussSum [84] software. All theoretical calculations were carried out using the Gaussian 03 program package [85].

Results and discussion

Properties of Cu(IDB)Cl_2 complex

To verify the theoretical models employed in the present calculations, we first calculated the properties of the Cu(IDB)Cl_2 complex based on the available experimental data obtained [79]. The optimized geometry of the Cu(IDB)Cl_2 complex represents an approximate C_{2v} symmetry. The computational results for the selected bond lengths and angles of the complex are shown in Table 2 along with the available experimental data. As one can see from Table 2, most calculated geometry parameters for Cu(IDB)Cl_2 complex agree with those determined by X-ray diffraction. Especially, the optimized parameters in the solvent are more consistent with the experimental data than those in the gas phase. Therefore, the following discussion about the properties of geometries, spectra and molecular orbitals will be focused on the optimized geometry in the solvent. In detail, the calculated Cu-N bond lengths (Å) are larger by percentage of 2.2 than those in the experiment [79]. The other bond lengths are very well reproduced. The computed angles (°) are larger by percentage of 0.9 than those in the experiment [79]. At the same time, the main C-C (N) bond-lengths of ligand skeletons in the complexes approach the standard bond-length (1.40 Å) [24]. So it may be deduced that the results of the full geometry optimization in the solvent are reliable. However, the computed bond length of 2.171 Å for Cu-N38 is much longer by 0.155 Å than those for Cu-N34 and Cu-N36. Nevertheless, such difference for the experimental value is only 0.041 Å. It could be explained by the fact that the hybridization mode of sp^3 for N38 is different from sp^2 for N34 and N36, which makes N38 form a tetrahedral structure. Furthermore, the interactions of Cu-N34 and Cu-N36 are more likely to approach a double bond; the interaction of Cu, however, with N38 is more likely to approach a single bond. That is to say, Cu-N38 bond is longer than the other two.

The TD-DFT method has been used to evaluate the excitation energies and oscillator strengths of the electronic excitations, which include all allowed singlet-singlet electron transitions in the UV and visible region (200–320 nm)

Table 1 Ground-state multiplicities and first-excited energies (kcal mol^{-1}) for M(IDB)Cl_2 complexes

	Mn	Fe	Co	Ni	Cu	Zn
Ground-state multiplicity	2	3	2	1	2	1
First-excited energy	24.6	11.1	39.7	8.6	74.8	77.2

Table 2 Selected computed bond lengths (Å) and angles (°) of Cu(IDB)Cl_2

Parameters	Gas[a]	Solvent[b]	Expt.[f]
Cu-N34	2.046	2.016	1.980
Cu-N36	2.046	2.016	1.988
Cu-N38	2.464	2.171	2.025
Cu-Cl17	2.326	2.405	2.266
Cu-Cl18	2.400	2.605	2.603
(C-C)m[c]	1.397	1.399	1.382
(C-N)m[d]	1.364	1.364	1.358
N34- Cu-N36	151.3	159.7	158.9
N34- Cu-N38	75.8	79.9	78.9
N36- Cu-N38	75.8	79.8	80.4
N38-Cu-Cl18-Cl17	180.0	179.9	178.0
N36-Cu-N34-Cl17	113.2	141.1	143.4

[a] and [b] express respectively optimized geometry parameters in the gas phase and in the solvent. [c] and [d] express the main bond lengths of ring skeleton of the IDB ligand. [f] is taken from ref. [79]

of the spectrum, for $Cu(IDB)Cl_2$ complex. This investigation with the corresponding solvent is comparable with the experimental data demonstrated by the previous studies [67, 86], and is helpful in assigning the electronic transition characteristics to the experimental absorption bands in more detail. The intensity of absorption band is evaluated as the oscillator strength (*f*) calculated in the dipole length representation. As is well known, the oscillator strengths are strongly dependent on the theoretical models. Therefore, three different exchange-correlation functionals, i.e., B3LYP, PW91 and PBE, were employed to investigate the optical absorption properties of the studied complex. The simulated UV spectra (200–320 nm) of $Cu(IDB)Cl_2$ with the three calculation models along with the experimental results [79] are presented in Fig. 2. As shown in Fig. 2, it is obvious that the UV spectrum of $Cu(IDB)Cl_2$ (as shown in Fig. 2(a)) simulated by B3LYP is more consistent with the experimental UV spectrum than those by PW91 and PBE. The computed absorption spectral energies, oscillator strengths (*f*) of the electronic transitions, and wavelengths with the B3LYP model along with the corresponding experimental data are also given in Table 3. The following discussions are mainly focused on the computational results by B3LYP method. It is observed from Table 3 that there are three strong transitions in the ultraviolet region, which are located at 203 nm (f=0.6356) for the first band, 237 nm (f=0.0598) and 250 nm (f=0.2266) for the second one, and 270 nm (f=0.2118) for the third one. It is theoretically assigned that the first absorption band at 203 nm presents the main ^{1}LLCT (ligand-to-ligand charge transfer) characteristics [87] of $\pi_L \rightarrow \pi_L^*$ transfer and the part ^{1}LMCT (ligand-to-metal charge transfer) characteristics of $\pi_L \rightarrow d_{Cu}^*$ transfer; that the second absorption band ranging from 237 nm to 250 nm presents mostly ^{1}LLCT characteristics. The

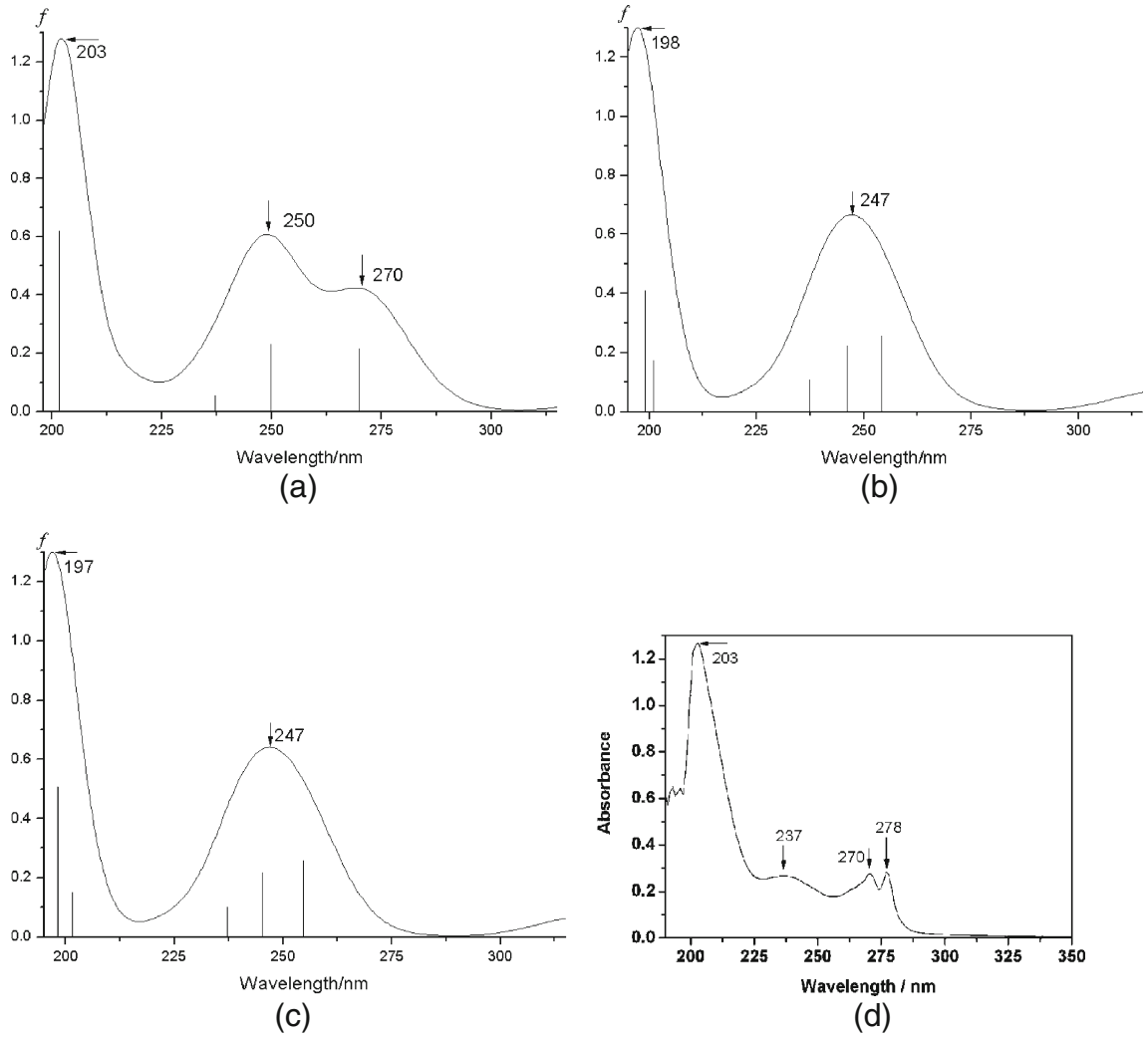

Fig. 2 Simulated UV spectra of $Cu(IDB)Cl_2$ in solvent using three DFT methods, (**a**) B3LYP, (**b**) PW91, and (**c**) PBE along with (**d**) experimental spectrum in ref. [79]

Table 3 Calculated excitation energies (*eV*, *nm*), oscillator strengths (*f*), and transition characters for $Cu(IDB)Cl_2$

λ_{expt} (*nm*)[a]	λ_{cal} (nm)	E/eV	f[b]	transitions	character
203	203	6.12	0.6356	H → L + 2 (25%)[c] H-3 → L + 4 (24%) H-1 → L + 3 (9%)	LLCT
237	237	5.23	0.0598	H-2 → L + 1 (42%) HOMO → L + 1 (23%)	LLCT
	250	4.96	0.2266	H-2 → L + 1 (38%) HOMO→ LUMO (15%) H-3 → L + 1 (13%)	LLCT
270, 277	270	4.59	0.2118	H-10 → LUMO (81%)	LMCT

[a] is taken from ref. [79]. [b] Oscillator strengths for $f<0.05$ are not list. [c] The percentage of contributions to wave functions of excited states are given in parentheses.

calculated spectra of other complexes will be presented and discussed in detail in Absorption spectra section. Summarily, the calculated geometry and spectroscopy information for $Cu(IDB)Cl_2$ complex are mostly consistent with the experimental results, supporting that the theoretical model and calculation levels used in the present work are suitable and reliable.

Properties of $M(IDB)Cl_2$ complexes

Geometries

The systematic studies on the geometries of transition metal complexes, $M(IDB)Cl_2$ (M = Mn, Fe, Co, Ni and Zn), in the same period were carried out at the same theoretical level with methanol solvent. The optimized geometries diagram of these complexes is shown in Fig. 1(b). The selected bond lengths and angles of these optimized complexes are listed in Table 4. It is clear from the calculated results that the electronic structures of the central metal cations could affect the geometries of complexes. The five-coordinated pattern of the center metal cation connecting the ligands in each of the studied complexes represents mostly an approximate trigonal bipyramidal structure. The two chlorine anions set at the axial position of trigonal bipyramid; and the three nitrogen atoms of IDB are located in the plane of trigonal bipyramid. However, the geometries of the complexes can be changed from the distorted trigonal bipyramidal structure to the square pyramidal one with the variations of electronic properties of the center metal cations. Namely, the geometries of Mn^{2+} and Co^{2+} complexes tend to the trigonal bipyramidal structures, and those of Fe^{2+}, Ni^{2+}, $Cu^{2+}$and Zn^{2+} complexes mostly approach to square pyramidal geometries.

Table 4 Selected calculated bond lengths (Å), angles (°) and coordination energies (kcal mol^{-1}) for the complexes

Parameter	$Mn(IDB)Cl_2$	$Fe(IDB)Cl_2$	$Co(IDB)Cl_2$	$Ni(IDB)Cl_2$	$Zn(IDB)Cl_2$
M-N34	2.099	2.006	1.957	1.916	2.195
M-N36	2.101	2.007	1.958	1.916	2.195
M-N38	2.097	2.099	2.084	2.048	2.299
M-Cl17	2.427	2.395	2.403	2.453	2.404
M-Cl18	2.451	2.476	2.487	2.560	2.415
(C-C)m[a]	1.399	1.399	1.399	1.398	1.399
(C-N)m[a]	1.364	1.364	1.363	1.364	1.364
N34-M-N36	159.8	162.2	164.3	164.7	146.4
N34-M-N38	80.0	81.1	82.3	82.7	74.0
N36-M-N38	79.9	81.1	82.1	82.7	73.9
N38-M-Cl18-Cl17	180.0	179.7	180.0	179.9	180.0
N36-M-N34-Cl17	97.1	136.9	128.6	145.5	120.3
Coordination Energy	536.52 664.87[b]	676.31	681.12	706.49	623.14

[a]: main bond lengths of ring skeleton of the IDB ligand. [b]: coordination energy for $Cu(IDB)Cl_2$.

Coordination stabilities

To discuss theoretically the coordination stabilities (S) of the investigated complexes, for the procedure of

$$M^{2+} + 2Cl^{-} + IDB \rightarrow M(IDB)Cl_2$$

we define the coordination energy, ΔE [63, 88], of a complex as follows:

$$\Delta E = E_{M2+} + 2E_{Cl-} + E_{IDB} - E_{M(IDB)Cl2} \quad (1)$$

where E_{M2+}, E_{Cl-}, E_{IDB} and $E_{M(IDB)Cl2}$ are the energies of M^{2+}, Cl^{-}, IDB and $M(IDB)Cl_2$, respectively. An identical computational method with gas phase was used to calculate the energies for these complexes and corresponding ions involved in the Eq. (1). According to Eq. (1), a positive value of ΔE represents that the corresponding complex is energetically stable. Moreover, the greater the coordination energy ΔE is, the more stable the complex is.

The computational coordination energies are shown in Table 4. The trend of coordination stabilities (S) for these complexes is in the order of S(Ni) > S(Co) > S(Fe) > S(Cu) > S(Zn) > S(Mn) with 706.49 kcal mol^{-1} for Ni, 681.12 kcal mol^{-1} for Co, 676.31 kcal mol^{-1} for Fe, 664.87 kcal mol^{-1} for Cu, 623.14 kcal mol^{-1} for Zn and 536.52 kcal mol^{-1} for Mn (see Table 4). These results indicate that metal center cations bind strongly to the IDB and chlorine ligands. It is obvious that the stabilities of Fe, Co and Ni complexes belonging to VIII family are higher than those for Cu, Zn and Mn complexes. The structural characteristics that the bond lengths of metal ions and N atoms of the IDB ligand for Cu, Zn and Mn complexes are longer than those of Fe, Co and Ni complexes supports this observation.

Electronic properties

The noncovalence or hyperconjugated interactions are estimated by the NBO method [89] as the second-order perturbation interaction energy, $E(2)$, between the occupied molecular orbitals (donor, i) and the neighboring unoccupied molecular orbitals (acceptor, j). The $E(2)$ called stabilization energy associates with the delocalization occurred (2e stabilization) between the donor NBO (i) and the acceptor NBO (j), and can be evaluated from the following equation:

$$E(2) = \Delta E_{ij} = q_i \cdot F^2(i,j) / (\varepsilon_j - \varepsilon_i) \quad (2)$$

where, q_i is the ith donor orbital occupancy; ε_i and ε_j are the diagonal elements (orbital energies); $F(i, j)$ is the off-diagonal elements associated with NBO Fock matrix element [90]. The greater the ΔE_{ij} value is, the stronger the interaction between an electron donor and acceptor is. Such energy analysis provides the assignment of orbital contribution to stabilizing these complex structures. To evaluate the contribution from the orbital interactions between the central metal cations and ligand anions, the NBO second-order perturbation analysis for these complexes was carried out at the same computational level based on the optimized geometries. The calculated results indicated that the orbital interactions depend greatly on the electronic properties of central transition metal cations. The obtained stabilization energies from the $n_N \rightarrow d_M^*$ orbital interactions are listed in Table 5. Since there are three nitrogen atoms N34, N36 and N38 connecting with the center metal cation in each complex, the value of interactions between a metal cation and N anions in one

Table 5 Second-order perturbation interaction energies of the complexes (kcal mol^{-1})

$Mn(IDB)Cl_2$ Donor → Acceptor	S. E.[a]	$Co(IDB)Cl_2$ Donor → Acceptor	S. E.	$Cu(IDB)Cl_2$ Donor → Acceptor	S. E
LP1N34→LP*3Mn39	12.90	LP1N34→LP4Co39	22.49	LP1N34→LP*5Cu39	12.64
LP1N34→LP*4Mn39	13.37	LP1N34→LP*5Co39	39.93	LP1N34→LP*6Cu39	43.33
LP1N36→LP*3Mn39	12.96	LP1N34→LP*6Co39	21.27	LP1N36→LP*5Cu39	12.60
LP1N36→LP*4Mn39	13.30	LP1N36→LP4Co39	22.44	LP1N36→LP*6Cu39	43.32
LP1N38→LP*5Mn39	20.81	LP1N36→LP*5Co39	39.80	LP1N38→LP*5Cu39	8.47
$Fe(IDB)Cl_2$ Donor → Acceptor	S. E.	LP1N36→LP*6Co39	21.25	LP1N38→LP*6Cu39	19.67
		LP1N38→LP4Co39	5.26	LP*6Cu39→RY*1N34	4.72
LP1N34→LP*3Fe39	22.20	LP1N38→LP*5Co39	12.64	LP*6Cu39→RY*1N36	4.71
LP1N34→LP*4Fe39	14.77	LP1N38→LP*6Co39	31.03		
LP1N34→LP*5Fe39	22.01	$Ni(IDB)Cl_2$ Donor → Acceptor	S. E.	$Zn(IDB)Cl_2$ Donor → Acceptor	S. E.
LP1N34→LP*6Fe39	16.27				
LP1N36→LP*3Fe39	22.05	LP1N34→LP*5Ni39	45.10	LP1N34→LP*6Zn39	25.23
LP1N36→LP*4Fe39	14.84	LP1N34→LP*6Ni39	40.97	LP1N36→LP*6Zn39	25.21
LP1N36→LP*5Fe39	21.87	LP1N36→LP*5Ni39	45.21	LP1N38→LP*6Zn39	14.86
LP1N36→LP*6Fe39	16.28	LP1N36→LP*6Ni39	41.05		
LP1N38→LP*4Fe39	11.43	LP1N38→LP*5Ni39	19.22		
LP1N38→LP*5Fe39	16.96	LP1N38→LP*6Ni39	25.67		
LP1N38→LP*6Fe39	17.59				

[a]: stabilization energy.

complex should be the sum of $n_N \rightarrow d_M^*$ orbital interactions for all three N atoms. In the NBO analysis, the natural bond orbitals are first defined for each covalent bond, lone pair, and antibonding orbital by using the obtained molecular orbitals; and the orbital interaction energies (i.e., the NBO second-order perturbation energies) are subsequently analyzed for all possible combinations of the two natural bond orbitals. It can be seen from the NBO analysis that the interactions between the lone pairs (n_N) of N atom ligands and the antibonding orbitals (d_M^*) of center metal cation (M) contribute significantly to the stabilization of the complex. The contribution of interaction of N34 or N36 with the metal cation in these complexes is larger than that of N38, due to N38 connecting to two pentagons with large steric tension and less electron donation, which is supported by the calculated geometry characteristics discussed above. Moreover, the orbital interactions between the metal ions and N atoms for the series of $M(IDB)Cl_2$ (M = Mn, Fe and Zn) complexes are smaller than those for M = Cu, Ni and Co complexes. Namely, the maximum stabilization energies for Mn, Fe and Zn complexes range up to 20.81, 23.04 and 25.23 kcal mol^{-1}, respectively; those for Cu, Co and Ni complexes are 43.33, 39.93 and 45.21 kcal mol^{-1}, respectively. These results are consistant with the small coordination energies for Mn and Zn complexes and large coordination energies for Ni and Co ones. However, the contribution of chlorine ligands to stabilization of complex does not present significant difference for various studied complexes.

According to the natural orbital population analysis (NPA), the net charge populations on some key atoms of $M(IDB)Cl_2$ complexes are given in Table 6. As one can see from Table 6, the charge populations on the central metal cations have been greatly influenced by metal electronic properties and coordination structures. The net charge populations on the Mn, Fe, Co, Ni, Cu and Zn cations for the corresponding complexes are 1.01, 1.50, 1.01, 1.03, 0.94 and 1.63, respectively. It is obvious that the charges localized at Fe and Zn cations are larger than those at others, which can be explained by the fact that Zn cation in the complex with full occupied d^{10} configuration and Fe cation with two parallel electrons occupying higher *d* orbitals are all unfavorable to accept other electrons from donors. Although the relative large positive charges localize at Zn and Fe cations in the corresponding complexes, such charge does not considerably increase the coordination stabilities of the complexes. The reasons for that may come from the coordination stabilities influenced by the whole electronic properties of the complexes with the ligands, atomic orbitals and polarity of the complexes, not only by the charges of metal cations.

Table 6 NBO charge populations at key atoms of the studied complexes

Complex	M39	N34	N36	N38	Cl17	Cl18
$Mn(IDB)Cl_2$	1.01	−0.29	−0.29	−0.33	−0.39	−0.39
$Fe(IDB)Cl_2$	1.50	−0.29	−0.29	−0.34	−0.37	−0.39
$Co(IDB)Cl_2$	1.01	−0.28	−0.28	−0.33	−0.40	−0.41
$Ni(IDB)Cl_2$	1.03	−0.55	−0.55	−0.68	−0.84	−0.87
$Cu(IDB)Cl_2$	0.94	−0.26	−0.26	−0.31	−0.37	−0.44
$Zn(IDB)Cl_2$	1.63	−0.68	−0.68	−0.76	−0.89	−0.90

Energies of the molecular orbitals

Previous studies have indicated that a DNA molecule and a transition metal complex are an electron-donor and an electron-acceptor [79, 91], respectively. The positive charges localized at the center metal ions for the metal complexes through the above NPA analysis also support the characteristics of electron-acceptors of metal complexes. According to the frontier molecular orbital theory [92], the lower the LUMO energy of the complex is, the easier the acceptance of electrons from the HOMO of DNA base pairs is, the stronger the binding of complex to DNA molecule is. The large population of ligands on LUMO of these complexes can be favorable to the orbital interaction between the complexes and DNA. Therefore, the DNA-binding abilities of the complexes can be possibly evaluated by the frontier molecular orbital interactions.

The stereographs of calculated LUMOs for the complexes as electron-acceptors are depicted in Fig. 3. It can be seen from Fig. 3 that the components of LUMOs of the complexes come mainly from the *d* orbitals of central metal cations and the *p* orbitals of chlorine anions, except for Mn and Zn complexes. However, the LUMOs of the Mn and Zn complexes are mainly contributed by the p_z orbitals of C and N of the IDB ligand. Considering the interaction of complex with DNA from molecular interaction, the contribution of the chlorine ligands to LUMO is much preferable to that of the IDB ligand as an electron-acceptor, which leads to the fact that the DNA affinities of the Fe, Co, Cu and Ni complexes are higher than those of the Mn and Zn complexes. For a simple comparison, a schematic representation of energy levels of some frontier molecular orbitals for these complexes is shown in Fig. 4. It is predicted from the LUMO's energies of the complexes in Fig. 4 that the binding affinities (*A*) of complexes are in the order of $A(Zn) < A(Mn) < A(Fe) \approx A(Co) < A(Ni) < A(Cu)$. For example, the ε_{LUMO} (−3.8243 eV) of the copper complex is the lowest one among these complexes, which means that the DNA affinity of copper complex would be the largest in all complexes studied. It is very interesting to note that the coordination stabilities are of approximately similar trend as their DNA affinity order for these

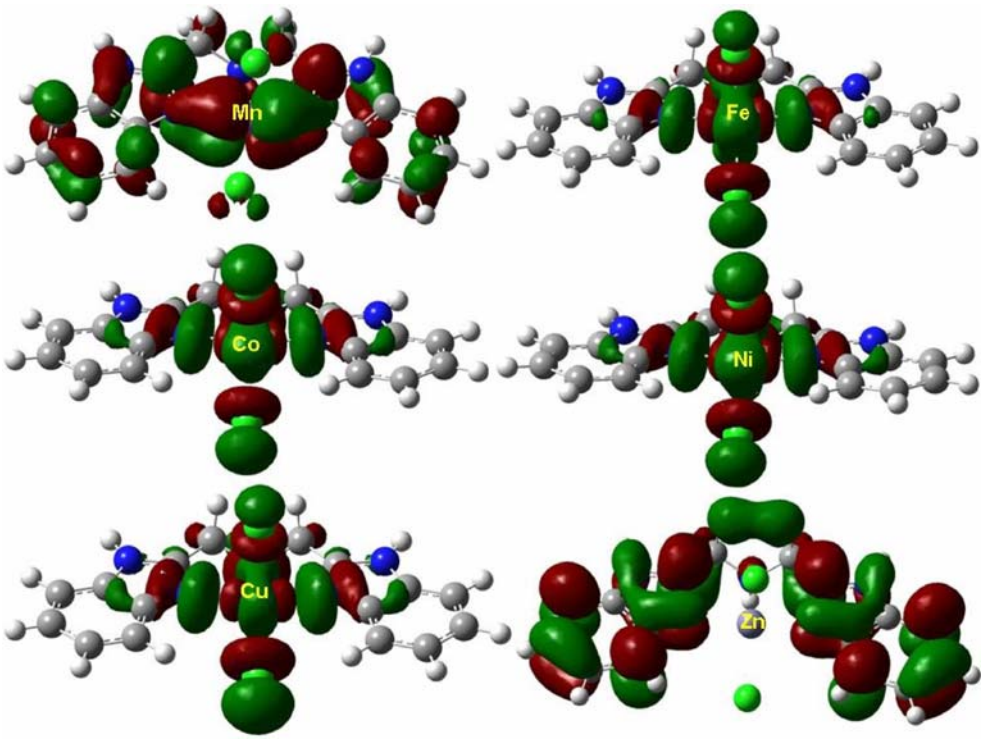

Fig. 3 LUMOs of $M(IDB)Cl_2$ (M = Mn, Fe, Co, Ni, Cu and Zn) complexes

complexes with the exceptions for the Cu complex and a slight switch between Mn and Fe complexes.

Absorption spectra

The absorption spectra of the $M(IDB)Cl_2$ (M = Mn, Fe, Co, Ni and Zn) complexes calculated by using the TD-DFT/B3LYP method in methanol solvent are shown in Fig. 5, except for Cu complex discussed in the first section. The computed absorption spectral energies, oscillator strengths (*f*) of the electron transition and wavelengths are given in Table 7. For the considered energy range, the spectra of the $M(IDB)Cl_2$ (M = Mn, Fe, Co, Ni and Zn) complexes present two bands as labeled "band I" around 187~210 nm and "band II" around 250 nm. The intensity of band I is larger than that of band II. It is conformed from the transition orbital analysis that band I around 187~210 nm for the calculated complexes represents the dominant ^{1}LLCT (ligand-to-ligand charge transfer, $\pi_L \rightarrow \pi_L^*$ transitions) and part ^{1}LMCT (ligand-to-metal charge transfer,

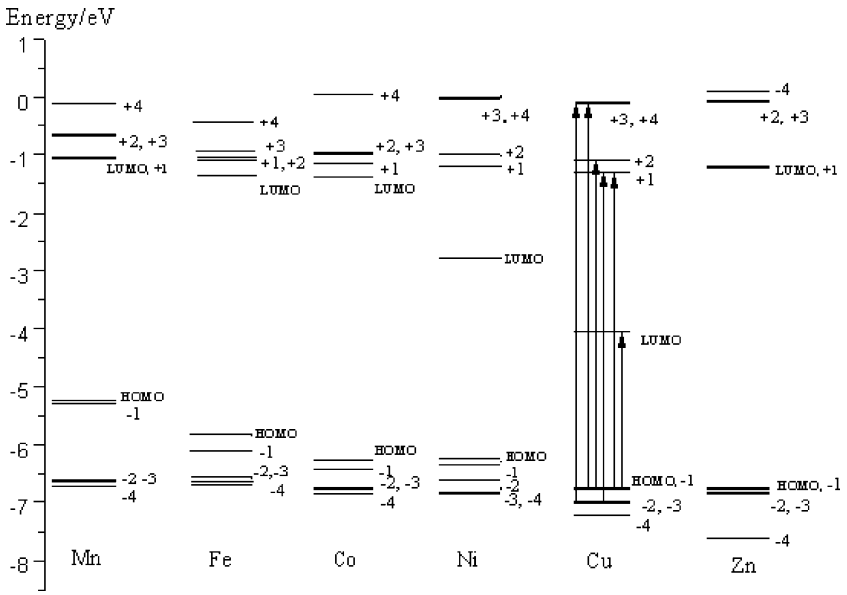

Fig. 4 Schematic representation of energies and transitions of some frontier molecular orbitals for $M(IDB)Cl_2$ complexes

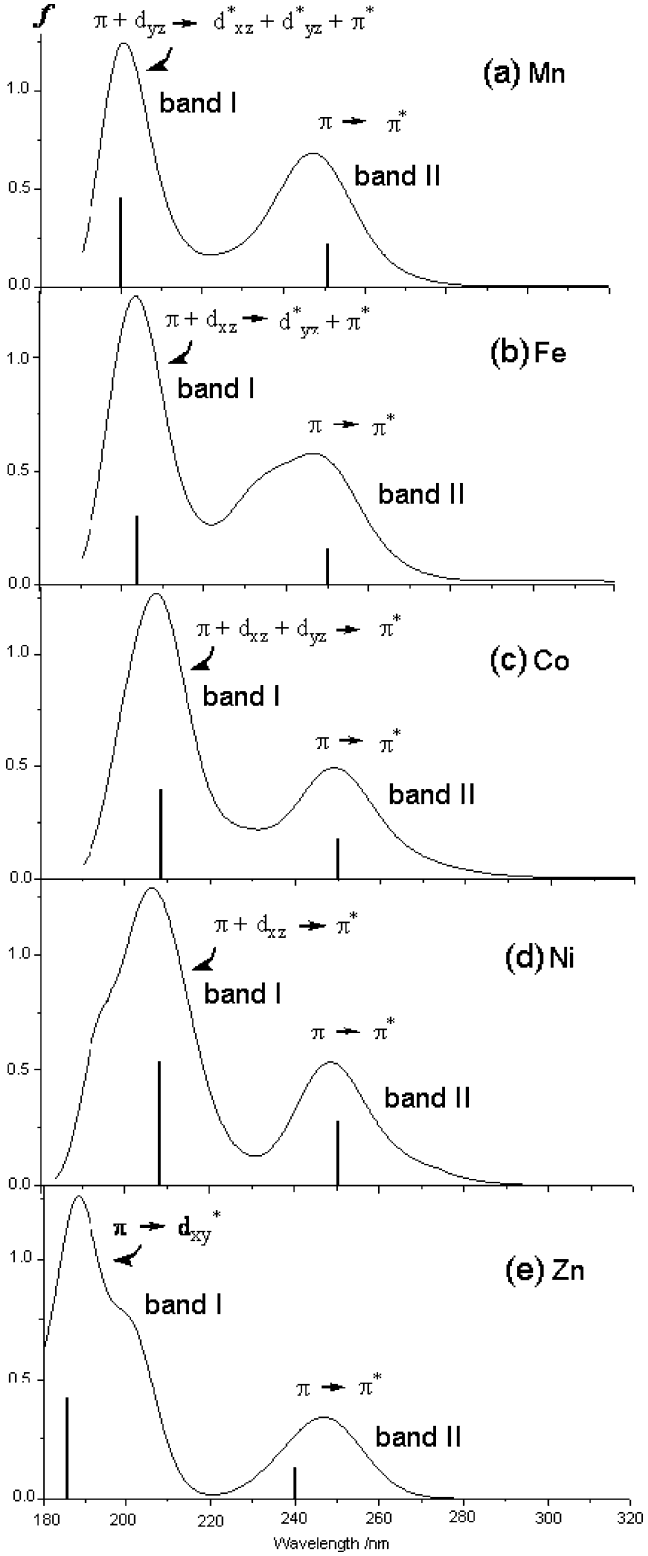

Fig. 5 Simulated UV spectra of $M(IDB)Cl_2$ in solvent along with electronic transition types

Table 7 Calculated excitation energies (*eV*, *nm*) and oscillator strengths (*f*) for the complexes

$M(IDB)Cl_2$	λ (*nm*)	*E* /eV	*f*	transitions
Mn	200	6.20	0.4474	H-2 → L + 7 (14%)
				H-2 → L + 5 (14%)
				H-2 → L + 7 (12%)
				H-3 → L + 5 (10%)
				H-4 → L + 6 (7%)
	251	4.94	0.1867	H-5 → L (33%)
				H-4 → L + 1 (21%)
				H-4 → L + 1 (8%)
				H-5 → L + 2 (7%)
Fe	205	6.05	0.2774	H-3 → L + 6(46%)
				H-3 → L + 3 (6%)
				H-2 → L + 6 (6%)
	250	4.96	0.1538	H → L + 2 (40%)
				H-2 → L (8%)
				H-7 → L + 2 (6%)
				H-2 → L + 4 (5%)
Co	210	5.90	0.3821	H → L + 4 (48%)
				H-1 → L + 4 (18%)
				H-6 → L + 3 (12%)
	250	4.96	0.1775	H-3 → L + 1 (47%)
				H-1 → L + 4(7%)
				H-5 → L + 2 (6%)
				H-2 → L + 5 (6%)
Ni	209	5.89	0.5115	H-10→ L + 1 (31%)
				H-2 → L + 3 (16%)
				H-2 → L + 5 (13%)
				H → L + 7 (10%)
	250	4.96	0.2597	H-4 → L + 1 (61%)
				H-5 → L + 2 (15%)
				H-2 → L + 3 (8%)
Zn	187	6.63	0.3976	H-1 → L + 5 (25%)
				H-2 → L + 3 (17%)
				H-3 → L + 2 (16%)
				H-1 → L + 4 (12%)
	240	5.16	0.1288	H-1 → L (77%)
				H-3 → L (6%)

$\pi_L \rightarrow d_M^*$ transitions) characteristics. The wavelength of dominant adsorption peaks for various complexes presents certain difference due to the band I including partly the ligand-to-metal electron transitions. The adsorption peak wavelength of band I for $Zn(IDB)Cl_2$ complex represents an obvious blue-shift to 187 nm compared with those of other complexes around 210 nm, due to the $\pi_L \rightarrow d_M^*$ transitions included in this band, and the d_M^* orbital energy being higher than that of π_L^* orbital for $Zn(IDB)Cl_2$. In addition, there are little blue-shifts to 205 nm for Mn and Fe complexes with part $\pi_L \rightarrow d_M^*$ transitions. On the other hand, the band II around 250 nm for all calculated complexes presents the excitation characteristics of ^{1}LLCT type. The adsorption peak wavelengths of band II for all

these complexes locate at mostly the same position around 250 nm, except for $Zn(IDB)Cl_2$ complex with little blue-shift to 240 nm caused by its symmetric electronic configuration (d^{10}). In addition, the HOMO energy of $Zn(IDB)Cl_2$ complex is the lowest in all studied complexes, which leads also to large excited energy for the electronic transitions.

Conclusions

The electronic structures, UV absorption spectra, and DNA-binding properties yielded by molecular orbital energies for the series of the complexes, $M(IDB)Cl_2$ (M = Mn, Fe, Co, Ni, Cu and Zn), have been studied by using the DFT/B3LYP and TD-DFT/B3LYP methods at the 6-311G** + LanL2DZ level of theory with PCM solvent model. The calculated results indicate the geometries of the complexes can be changed from the distorted trigonal bipyramidal structure to the square pyramidal one with the variations of electronic properties of the center metal cations. The calculated coordination energies of the $M(IDB)Cl_2$ complexes demonstrate the order of coordination stability of S(Ni) >> S(Co) > S(Fe) > S(Cu) > S(Zn) > S(Mn). The DNA-binding affinities yielded by the LUMO energies of these complexes are in the order of $A(Zn) < A(Mn) < A(Fe) \approx A(Co) < A(Ni) < A(Cu)$. It can be estimated further that the complex with large coordination stability generally presents the strong DNA-binding ability for the studied complexes. Adsorption spectral bands were theoretically simulated lying in the range of 180–320 nm in methanol solvent. The characteristics of electron transitions of the complexes with ^{1}LLCT and ^{1}LMCT types for band I and ^{1}LLCT for band II are also assigned.

Acknowledgements This work is supported by the National Natural Science Foundation of China (No. 20673011, 20631020, and 20771017) and the Major State Basic Research Development Programs (grant No. G2004CB719900). We also acknowledge computing resources provided by the HPSC of Beijing Normal University.

References

1. Barton JK, Danishefsky A, Goldberg J (1984) J Am Chem Soc 106:2172–2176. doi:10.1021/ja00319a043
2. Yaumei H, Barton J (1988) Proc Natl Acad Sci USA 85:1339–1343. doi:10.1073/pnas.85.5.1339
3. Barton JK (1986) Science 233:727–734. doi:10.1126/science.3016894
4. Hartshorn RM, Barton JK (1992) J Am Chem Soc 114:5919–5925. doi:10.1021/ja00041a002
5. Hiort C, Lincoln P, Norden B (1993) J Am Chem Soc 115:3448–3454. doi:10.1021/ja00062a007
6. Metcalfe C, Thomas JA (2003) Chem Soc Rev 32:215–224. doi:10.1039/b201945k
7. Friedman AE, Chambron JC, Sauvage JP, Turro NJ, Barton JK (1990) J Am Chem Soc 112:4960–4962. doi:10.1021/ja00168a052
8. Olson EJC, Hu D, Hormann A, Jonkman AM, Arkin MR, Stemp EDA, Barton JK, Barbara PF (1997) J Am Chem Soc 119:11458–11467. doi:10.1021/ja971151d
9. Jenkins Y, Barton JK (1992) J Am Chem Soc 114:8736–8738. doi:10.1021/ja00048a077
10. Arounaguiri S, Maiya BG (1999) Inorg Chem 38:842–843. doi:10.1021/ic981109z
11. Liu XW, Li J, Li H, Zheng KC, Chao H, Ji LN (2005) J Inorg Biochem 99:2372–2380
12. Ji LN, Zou XH, Liu JG (2001) Coord Chem Rev 216–217:513–536. doi:10.1016/S0010-8545(01)00338-1
13. Grimm GN, Boutorine AS, Lincoln P, Nordén B, Hélène C (2002) ChemBioChem 3:324–331. doi:10.1002/1439-7633(20020402)3:4<324::AID-CBIC324>3.0.CO;2-7
14. Delaney S, Pascaly M, Bhattacharya PK, Han K, Barton JK (2002) Inorg Chem 41:1966–1974. doi:10.1021/ic0111738
15. Maheswari PU, Palaniandavar M (2004) J Inorg Biochem 98:219–230. doi:10.1016/j.jinorgbio.2003.09.003
16. Ruba E, Hart JR, Barton JK (2004) Inorg Chem 43:4570–4578. doi:10.1021/ic0499291
17. Sigman DS, Mazumder A, Perrin DM (1993) Chem Rev 93:2295–2316. doi:10.1021/cr00022a011
18. Claussen CA, Long EC (1999) Chem Rev 99:2797–2816. doi:10.1021/cr980449z
19. Decker A, Chow MS, Kemsley JN, Lehnert N, Solomon EI (2006) J Am Chem Soc 128:4719–4733. doi:10.1021/ja057378n
20. Maiti D, Woertink JS, Vance MA, Milligan AE, Sarjeant AAN, Solomon EI, Karlin KD (2007) J Am Chem Soc 129:8882–8892. doi:10.1021/ja071968z
21. Decker A, Rohde J-U, Klinker EJ, Wong SD, Lawrence Que J, Solomon EI (2007) J Am Chem Soc 129:15983–15996. doi:10.1021/ja074900s
22. Wang XY, Zhang J, Li K, Jiang N, Chen SY, Lin HH, Huang Y, Ma LJ, Yu XQ (2006) Bioorg Med Chem 14:6745–6751. doi:10.1016/j.bmc.2006.05.049
23. Kang JW, Dong SQ, Lu XQ, Su BQ, Wu HX, Sun K (2006) Bioelectrochemistry 69:58–64. doi:10.1016/j.bioelechem.2005.10.005
24. Zheng KC, Wang JP, Peng WL, Liu XW, Yun FC (2001) J Phys Chem A 105:10899–10905. doi:10.1021/jp0126560
25. Erkkila KE, Odom DT, Barton JK (1999) Chem Rev 99:2777–2795. doi:10.1021/cr9804341
26. Franklin SJ, Barton JK (1998) Biochemistry 37:16093–16105. doi:10.1021/bi981798q
27. Hastings CA, Barton JK (1999) Biochemistry 38:10042–10051. doi:10.1021/bi982039a
28. Xiong Y, Ji LN (1999) Coord Chem Rev 185–186:711–733. doi:10.1016/S0010-8545(99)00019-3
29. Marincola FC, Casu M, Saba G, Lai A, Lincoln P, Norden B (1998) Chem Phys 236:301–308. doi:10.1016/S0301-0104(98)00199-2
30. Lincoln P, Norden B (1998) J Phys Chem B 102:9583–9594. doi:10.1021/jp9824914
31. Coggan DZM, Haworth IS, Bates PJ, Robinson A, Rodger A (1999) Inorg Chem 38:4486–4497. doi:10.1021/ic990654c
32. Oyoshi T, Sugiyama H (2000) J Am Chem Soc 122:6313–6314. doi:10.1021/ja9919130
33. Bales BC, Pitie M, Meunier B, Greenberg MM (2002) J Am Chem Soc 124:9062–9063. doi:10.1021/ja026970z
34. Itoh Y, Hayashi H, Furutachi H, Matsumoto T, Nagatomo S, Tosha T, Terada S, Fujinami S, Suzuki M, Kitagawa T (2005) J Am Chem Soc 127:5212–5223. doi:10.1021/ja047437h
35. Geierstanger BH, Mrksich M, Dervan PB, Wemmer DE (1994) Science 266:646–650. doi:10.1126/science.7939719

36. Pratviel G, Bernadou J, Meunier B (1995) Angew Chem Int Ed Engl 34:746–749. doi:10.1002/anie.199507461
37. Uma V, Kanthimathi M, Subramanian J, Nair BU (2006) Biochim Biophys Acta 1760:814–819
38. Barton JK, Raphael AL (1984) J Am Chem Soc 108:2466–2468. doi:10.1021/ja00320a058
39. Kumar CV, Barton JK, Turro NJ (1985) J Am Chem Soc 107:5518–5523. doi:10.1021/ja00305a032
40. Shields TP, Barton JK (1995) Biochemistry 34:15049–45056. doi:10.1021/bi00046a010
41. Dupureur CM, Barton JK (1997) Inorg Chem 36:33–43. doi:10.1021/ic960738a
42. Sitlani A, Barton JK (1994) Biochemistry 33:12100–12108. doi:10.1021/bi00206a013
43. Jenkins Y, Friedman AE, Turro NJ, Barton JK (1992) Biochemistry 31:10809–10816. doi:10.1021/bi00159a023
44. Dupureur CM, Barton JK (1994) J Am Chem Soc 116:10286–10287. doi:10.1021/ja00101a053
45. Turro C, Bossmann SH, Jenkins Y, Barton JK, Turro NJ (1995) J Am Chem Soc 117:9026–9032. doi:10.1021/ja00140a020
46. Barton JK, Goldberg JM, Kumar CV, Turro NJ (1986) J Am Chem Soc 108:2081–2088. doi:10.1021/ja00268a057
47. Pyle AM, Rehmann JP, Meshoyrer R, Kumar CV, Turro NJ, Barton JK (1989) J Am Chem Soc 111:3051–3058. doi:10.1021/ja00190a046
48. Sigman DS, Graham DR, D'Aurora V, Stern AM (1979) J Biol Chem 254:12269–12272
49. Sigman DS (1986) Acc Chem Res 19:180–186. doi:10.1021/ar00126a004
50. Zhu YY, Su YW, Li XC, Wang Y, Chen GJ (2008) Chem Phys Lett 455:354–360. doi:10.1016/j.cplett.2008.03.004
51. Li C, Qiao R-Z, Wang Y-Q, Zhao Y-F, Zeng R (2008) Bioorg Med Chem Lett 18:5766–5770. doi:10.1016/j.bmcl.2008.09.074
52. Li C, Qiao R-Z, Zhao Y-F (2008) Int J Mass Spectrom 270:94–99. doi:10.1016/j.ijms.2007.10.011
53. Sundberg RJ, Martin RB (1974) Chem Rev 74:471–517. doi:10.1021/cr60290a003
54. Lombardy RL, Tanious FA, Ramachandran K, Tidwell RR, Wilson WD (1996) J Med Chem 39:1452–1462. doi:10.1021/jm9507946
55. Liu CL, Yu SW, Li DF, Liao ZR, Sun XH, Xu HB (2002) Inorg Chem 41:913–922. doi:10.1021/ic010302h
56. Vaidyanathan VG, Nair BU (2003) J Inorg Biochem 94:121–126. doi:10.1016/S0162-0134(02)00620-7
57. Liu C, Wang M, Zhang T, Sun H (2004) Coord Chem Rev 248:147–168. doi:10.1016/j.cct.2003.11.002
58. Zhou Q, Yang P (2006) Inorg Chim Acta 359:1200–1206. doi:10.1016/j.ica.2005.11.003
59. Teng MK, Usman N, Frederick CA, Wang AHJ (1988) Nucleic Acids Res 16:2671–2690. doi:10.1093/nar/16.6.2671
60. Parkinson JA, Barber J, Douglas KT, Rosamond J, Sharplest D (1990) Biochemistry 29:10181–10190. doi:10.1021/bi00496a005
61. Mei WJ, Liu J, Zheng KC, Lin LJ, Chao H, Li AX, Yun FC, Ji LN (2003) Dalton Trans 1352–1359. doi:10.1039/b212443b
62. Shi S, Liu J, Li J, Zheng KC, Huang XM, Tan CP, Chen LM, Ji LN (2006) J Inorg Biochem 100:385–395. doi:10.1016/j.jinorgbio.2005.12.005
63. Zheng KC, Wang JP, Shen Y, Peng WL, Yun FC (2002) J Chem Soc, Dalton Trans 1:111–116. doi:10.1039/b105266g
64. Li J, Xu LC, Chen JC, Zheng KC, Ji LN (2006) J Phys Chem A 110:8174–8180. doi:10.1021/jp0564389
65. Xu LC, Li J, Shen Y, Zheng KC, Ji LN (2007) J Phys Chem A 111:273–280. doi:10.1021/jp064189y
66. Pourtois G, Beljonne D, Moucheron C, Schumm S, Mesmaeker AK-D, Lazzaroni R, Bredas JL (2004) J Am Chem Soc 126:683–692. doi:10.1021/ja034444h
67. Nazeeruddin MK, De Angelis F, Fantacci S, Selloni A, Viscardi G, Liska P, Ito S, Takeru B, Gratzel M (2005) J Am Chem Soc 127:16835–16847. doi:10.1021/ja052467l
68. Pfletschinger A, Koch W, Schmalz HG (2001) Chem Eur J 7:5325–5332. doi:10.1002/1521-3765(20011217)7:24<5325::AID-CHEM5325>3.0.CO;2-S
69. Stoyanov SR, Villegas JM, Rillema DP (2002) Inorg Chem 41:2941–2945. doi:10.1021/ic0110629
70. Zheng KC, Liu XW, Deng H, Chao H, Yun FC, Ji LN (2003) J Mol Struct THEOCHEM 626:295–304. doi:10.1016/S0166-1280(03)00103-9
71. Jiang Q, Xiao N, Shi P, Zhu Y, Guoa Z (2007) Coord Chem Rev 251:1951–1972. doi:10.1016/j.ccr.2007.02.013
72. Becke AD (1993) J Chem Phys 98:5648–5652. doi:10.1063/1.464913
73. Lee C, Yang W, Parr RG (1988) Phys Rev B 37:785–789. doi:10.1103/PhysRevB.37.785
74. Stevens PJ, Devlin FJ, Chablowski CF, Frisch MJ (1994) J Phys Chem 98:11623–11627. doi:10.1021/j100096a001
75. Becke AD (1993) J Chem Phys 98:1372–1377. doi:10.1063/1.464304
76. Hay PJ, Wadt WR (1985) J Chem Phys 82:270–283. doi:10.1063/1.448799
77. Hay PJ, Wadt WR (1985) J Chem Phys 82:299–310. doi:10.1063/1.448975
78. Schäfer A, Huber C, Ahlrichs R (1994) J Chem Phys 100:5829–5835. doi:10.1063/1.467146
79. Liu CL, Zhou JY, Li QX, Wang LJ, Liao ZR, Xu HB (1999) J Inorg Biochem 75:233–240. doi:10.1016/S0162-0134(99)00037-9
80. Mierts S, Scrocco E, Tomasi J (1981) Chem Phys 55:117–129. doi:10.1016/0301-0104(81)85090-2
81. Glendening ED, Reed AE, Carpenter JE, Weinhold F. (included in the GAUSSIAN 03 package of programs), NBO Version 3.1
82. Bai B, Deng K, Yang J, Zhu Q (2003) J Chem Phys 118:9608–9613. doi:10.1063/1.1555091
83. Davidson ER (1975) J Comput Phys 17:87–94. doi:10.1016/0021-9991(75)90065-0
84. O'Boyle NM, Vos JG (2006) GaussSum 2.0, Dublin City University
85. Frisch MJ, Trucks GW, Schlegel HB, Scuseria GE, Robb MA, Cheeseman JR, Montgomery JA, Vreven JT, Kudin KN, Burant JC, Millam JM, Iyengar SS, Tomasi J, Barone V, Mennucci B, Cossi M, Scalmani G, Rega N, Petersson GA, Nakatsuji H, Hada M, Ehara M, Toyota K, Fukuda R, Hasegawa J, Ishida M, Nakajima T, Honda Y, Kitao O, Nakai H, Klene M, Li X, Knox JE, Hratchian HP, Cross JB, Bakken V, Adamo C, Jaramillo J, Gomperts R, Stratmann RE, Yazyev O, Austin AJ, Cammi R, Pomelli C, Ochterski JW, Ayala PY, Morokuma K, Voth GA, Salvador P, Dannenberg JJ, Zakrzewski VG, Dapprich S, Daniels AD, Strain MC, Farkas O, Malick DK, Rabuck AD, Raghavachari K, Foresman JB, Ortiz JV, Cui Q, Baboul AG, Clifford S, Cioslowski J, Stefanov BB, Liu G, Liashenko A, Piskorz P, Komaromi I, Martin RL, Fox DJ, Keith T, Al-Laham MA, Peng CY, Nanayakkara A, Challacombe M, Gill PMW, Johnson B, Chen W, Wong MW, Gonzalez C, Pople JA (2004) Gaussian 03 Gaussian, Inc., Wallingford CT
86. Angelis FD, Fantacci S, Selloni A, Nazeeruddin MK (2005) Chem Phys Lett 415:115–120. doi:10.1016/j.cplett.2005.08.044
87. Yamaguchi K, Koshino S, Akagi F, Suzuki M, Uehara A, Suzuki S (1997) J Am Chem Soc 119:5752–5753. doi:10.1021/ja963982+
88. Zheng KC, Liu XW, Wang JP, Yun FC, Ji LN (2003) J Mol Struct THEOCHEM 637:195–203. doi:10.1016/S0166-1280(03)00539-6
89. Reed AE, Curtiss LA, Weinhold F (1988) Chem Rev 88:899–926. doi:10.1021/cr00088a005
90. Davood NS, Maryam M, Farzad D (2006) J Mol Struct THEOCHEM 763:187–198. doi:10.1016/j.theochem.2006.01.032
91. Pogozelski WK, Tullius TD (1998) Chem Rev 98:1089–1107. doi:10.1021/cr960437i
92. Fukui K, Yonezawa T, Shingu H (1952) J Chem Phys 20:722–755. doi:10.1063/1.1700523